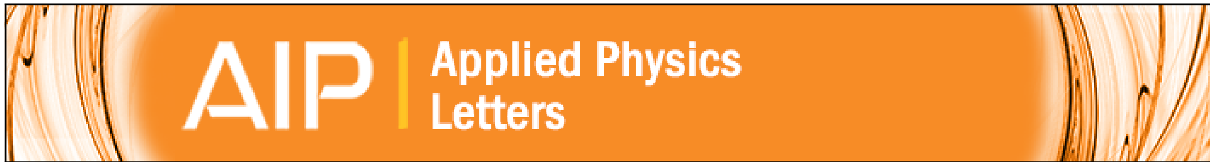

Sequential thermal treatments of SiC in NO and O 2 : Atomic transport and electrical characteristics

G. V. Soares, I. J. R. Baumvol, L. Hold, F. Kong, J. Han, S. Dimitrijev, C. Radtke, and F. C. Stedile

Citation: Applied Physics Letters **91**, 041906 (2007); doi: 10.1063/1.2763966
View online: http://dx.doi.org/10.1063/1.2763966
View Table of Contents: http://scitation.aip.org/content/aip/journal/apl/91/4?ver=pdfcov
Published by the AIP Publishing

Articles you may be interested in

Comparative study of thermally grown oxides on n -type free standing 3 C -SiC (001)
J. Appl. Phys. **106**, 044513 (2009); 10.1063/1.3204642

Effects of reoxidation on band alignment in N-incorporated SiON films as a function of sequential thermal annealing in NO and N H 3
Appl. Phys. Lett. **93**, 012901 (2008); 10.1063/1.2955835

Nitridation anisotropy in SiO 2⁄4 H – SiC
J. Appl. Phys. **97**, 074902 (2005); 10.1063/1.1863423

Density profiles and electrical properties of thermally grown oxide nanofilms on p -type 6H–SiC(0001)
Appl. Phys. Lett. **85**, 5580 (2004); 10.1063/1.1829385

Effects of nitridation and annealing on interface properties of thermally oxidized SiO 2 / SiC metal–oxide–semiconductor system
Appl. Phys. Lett. **76**, 3744 (2000); 10.1063/1.126769

AIP Applied Physics Reviews
NEW Special Topic Sections
NOW ONLINE
Lithium Niobate Properties and Applications: Reviews of Emerging Trends
AIP Applied Physics Reviews

Reuse of AIP Publishing content is subject to the terms at: https://publishing.aip.org/authors/rights-and-permissions. Download to IP: 143.54.44.137 On: Thu, 05 May 2016 19:14:47

Sequential thermal treatments of SiC in NO and O_2: Atomic transport and electrical characteristics

G. V. Soares[a]
PGMICRO, UFRGS, CP 15064 Porto Alegre, RS, Brazil 90501-970

I. J. R. Baumvol
CCET, Universidade de Caxias do Sul, Brazil 95070-560 and Instituto de Física, UFRGS, Porto Alegre, RS, Brazil 91509-900

L. Hold, F. Kong, J. Han, and S. Dimitrijev
Queensland Microtechnology Facility, Griffith University, Nathan, Queensland 4111, Australia and Griffith School of Engineering, Griffith University, Nathan, Queensland 4111, Australia

C. Radtke and F. C. Stedile
Instituto de Química, UFRGS, Porto Alegre, RS, Brazil 91509-900

(Received 29 May 2007; accepted 1 July 2007; published online 26 July 2007)

Sequential thermal oxidations and oxynitridations of SiC were performed using $^{18}O_2$ and NO. The resulting films were characterized by x-ray photoelectron spectroscopy, ion beam analyses, and capacitance-voltage measurements. The best electrical characteristics were obtained from films directly grown in NO. A subsequent oxidation in O_2 degraded the interface due to negative flatband-voltage shift, removal of N, and formation of C compounds, while a further annealing in NO brought the flatband shift in the *C-V* curves to rather moderate figures. This shift is related to competitive processes taking place during dielectric film formation which are discussed. © *2007 American Institute of Physics*. [DOI: 10.1063/1.2763966]

Silicon carbide (SiC) is an excellent wide-band-gap semiconductor for high power, temperature, and frequency electronic devices. However, the higher electronic interface state density (D_{it}) and the lower channel mobility of thermally grown SiO_2 films on SiC (SiO_2/SiC) when compared to SiO_2/Si, still prevent the wide application of SiC as a semiconductor material.[1,2] In order to reduce D_{it}, different postoxidation annealings (POAs) were already performed.[3–5] Among them, annealing in NO is considered the most effective one. It is well established that N is crucial on D_{it} reduction in SiO_2/SiC;[5–7] nevertheless, the actual role played by N in the passivation of electrical active defects in the SiO_2/SiC interface has remained elusive.[7,8] There are some relevant electrical and physicochemical aspects that still need to be clarified, such as (i) why oxides thermally grown on SiC substrates preannealed in NO present superior electrical characteristics when compared with their SiO_2/SiC (without N) counterparts, (ii) what are the differences between NO pre- and postoxidation annealings, and (iii) what the influences of an oxidation step before and after a NO step are. These crucial questions to understand NO electrical passivation of SiO_2/SiC-based metal-oxide-semiconductor (MOS) structures are addressed in the present letter by thermally growing dielectric films on SiC in different sequential oxynitridation and oxidation routes. After each processing step, analytical tools were employed to track the changes induced by this lastly performed step.

Silicon-faced (0001) *n*-type on-axis 6*H*-SiC samples were cleaned with the standard RCA process, etched in a 5% HF aqueous solution for 1 min, and loaded in the furnace. Two types of treatments were used in the preparation of samples. The $^{18}O_2$ treatment consisted of a thermal oxidation at 1100 °C for 1 h in a static atmosphere of 100 mbar of dry oxygen enriched to 97% in ^{18}O. The oxynitridation step (termed "NO") was performed by annealing the sample at 1170 °C for 2 h in a constant NO flow rate of 1 SLM (SLM denotes standard liter per minute). Different sequences of the precedent treatments gave rise to the following sets of films grown on SiC: $^{18}O_2$, NO, NO/$^{18}O_2$, $^{18}O_2$/NO, and NO/$^{18}O_2$/NO. The amount of N incorporated before and after the SiO_2 thermal growth step was determined in a previous work[9] to be around $\sim 10^{14}$ N/cm^2, mostly near the SiO_2/SiC interface. The use of the ^{18}O rare isotope (natural abundance of 0.2%) allows one to distinguish it from O incorporated in samples during air exposure and/or NO annealings. ^{18}O quantification was accessed by nuclear reaction analysis (NRA),[10] with a sensitivity of $\sim 10^{13}$ $^{18}O/cm^2$ and 5% accuracy. The areal density of ^{16}O was determined by Rutherford backscattering spectrometry in channeled geometry (c-RBS), with 10% accuracy.[10] X-ray photoelectron spectroscopy (XPS) was performed in an Omicron-EA125 station, using Mg $K\alpha$ radiation (1253.6 eV). MOS capacitors with aluminum gates (0.0025 cm^2) were fabricated on *n*-type 6*H*-SiC epitaxial layers with doping concentration of 2×10^{16} cm^{-3} to enable electrical characterization at 250 °C by high-frequency (10 kHz) capacitance-voltage (HFCV) measurements. At 250 °C, all interface traps from the upper half of the energy gap can respond within the measurement time employed. HFCV characteristics were obtained at the sweep rate of 0.1 V/s using a computer controlled HP4284A *LCR* meter.

Figure 1 shows Si 2*p* photoelectron energy regions at 45° [bulk sensitive mode (a)] and 25° [interface sensitive mode (b)] take-off angles for all sets of samples. A single component is identified in both modes for samples $^{18}O_2$ (□) at a binding energy E_b=104 eV, assigned to Si–O bonding in

[a]Electronic mail: gabriel.soares@ufrgs.br

Reuse of AIP Publishing content is subject to the terms at: https://publishing.aip.org/authors/rights-and-permissions. Download to IP: 143.54.44.137 On: Thu, 05 May 2016 19:14:47

 © 2007 American Institute of Physics

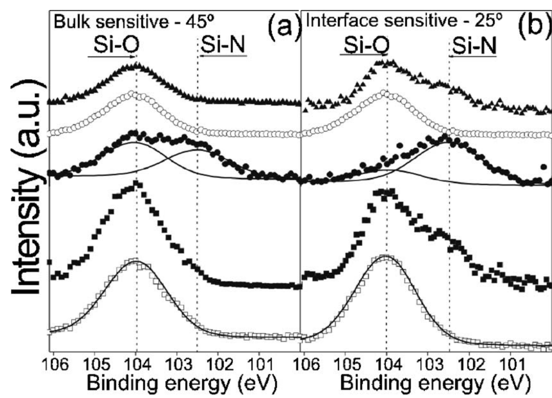

FIG. 1. Si 2*p* photoelectron spectra (a.u.=arbitrary units) at take-off angles of 45° [bulk sensitive (a)] and 25° [interface sensitive (b)] for SiC samples annealed in (from bottom to top): $^{18}O_2$ (□), $^{18}O_2$/NO (■), NO (●), NO/$^{18}O_2$ (○), and NO/$^{18}O_2$/NO (▲). Energy positions for Si–O and Si–N environments are indicated. Fittings are presented for samples $^{18}O_2$ and NO.

SiO_2. After POA in NO (samples $^{18}O_2$/NO—■), a second component is observed at E_b=102.5 eV in the interface sensitive mode. This component can be assigned[11] to Si–N bonding in silicon oxynitride, where N has O as a second neighbor. Since the component at 102.5 eV is not apparent in the bulk sensitive mode, one can say that N is incorporated mainly in the SiO_2/SiC interfacial region and that it is directly bonded to Si and probably to C as well. N incorporated in this region is proposed[12] to passivate electrically active C clusters and suboxides by the formation of Si–N and C–N bonds, although no evidence of C–N bonds was observed in the present work (from C 1*s* spectra, not shown). In the case of NO samples (●) the two components are observed in both modes, evidencing that this film is a silicon oxynitride. The intensity ratio of such components (Si–N/Si–O) at the two take-off angles points again to a higher concentration of Si–N bonds close to the dielectric/SiC interface. Spectra of NO/$^{18}O_2$ samples (○) present only one component, related to Si–O bonds (SiO_2), with no signal corresponding to Si–N bonds, indicating that the N concentration decreased below the sensitivity of XPS after $^{18}O_2$ annealing. When a further NO annealing is performed in NO/$^{18}O_2$ samples, yielding NO/$^{18}O_2$/NO samples (▲), N incorporation occurs in a similar way as in $^{18}O_2$/NO samples: there is incorporation of N in the interface region (formation of Si–N bonds), while no incorporation of N in the bulk of the film is observed.

Previous works[13,14] have reported N and O mobility during thermal oxynitridation in NO of thermally grown SiO_2 films on Si. They showed that during the NO process, besides incorporation of N near the SiO_2/Si interface, there is also atomic exchange between oxygen from the gas phase (NO) and oxygen from the SiO_2 film. In order to verify if this is also the case in SiC-based samples, we performed NRA and c-RBS analyses to determine ^{18}O and ^{16}O total amounts after each thermal annealing step. Figure 2 shows c-RBS spectra for all sets of samples. Table I presents ^{18}O and ^{16}O total amounts and film thicknesses determined using the relation 10^{15} O/cm^2 ~ 0.226 nm.[10] One notices that the c-RBS spectrum for $^{18}O_2$ samples (□) has only a signal corresponding to ^{18}O, apart from the C signal from the substrate. After the N^{16}O annealing (■ and Table I) there is a complete (within experimental sensitivity) isotopic exchange between ^{16}O from the gas phase and ^{18}O from the film. N

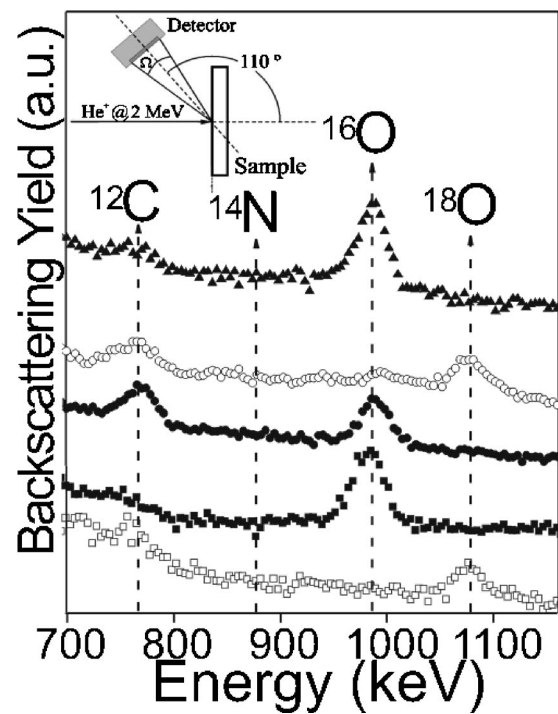

FIG. 2. c-RBS spectra of all samples using 2 MeV incident He^+ with detection of the scattered ions at 110°. Symbols are the same as in Fig. 1. Vertical lines correspond to the energy position of each isotope signal.

incorporation, which was made evident by XPS results above, remains below the detection limit of these c-RBS. Moreover, there is an increase in the oxide film thickness (Table I) as compared to $^{18}O_2$ samples, which is attributed to NO dissociation at high temperatures ($2NO \rightarrow N_2 + O_2$) yielding molecular oxygen that oxidizes the SiC substrate. When the gas sequence is inverted, besides N and O incorporation by direct reaction of NO with the SiC structure, there is also O isotope exchange, as can be seen by comparing the c-RBS spectra of NO (●) and NO/$^{18}O_2$ (○) samples (see also Table I). In addition to isotopic exchange, XPS results showed that there is also complete N removal from the film. An additional NO annealing of NO/$^{18}O_2$ samples induces once more O isotopic substitution (see ▲) and increase in the film thickness (Table I). The mechanisms of N and O incorporation in SiO_2/SiC appear to be very similar to the mechanisms governing the SiO_2/Si thermal treatment in NO.[13] Here, the mechanisms seem to be: (i) diffusion of NO molecules through the silica network without reacting with it; (ii) reaction of NO at the SiO_2/Si interface, incorporating N and O (promoting film growth); and (iii) O isotopic exchange mediated by the presence of network defects. Comparing the present results with those obtained for films on Si in a quan-

TABLE I. ^{18}O and ^{16}O total amounts, and film thicknesses determined by NRA and c-RBS for all sets of samples.

Samples	^{18}O (10^{15} at. cm^{-2})	^{16}O (10^{15} at. cm^{-2})	Thickness (nm)
$^{18}O_2$	22	⋯	5
$^{18}O_2$/NO	⋯	70	16
NO	⋯	32	7.5
NO/$^{18}O_2$	36	1	9
NO/$^{18}O_2$/NO	⋯	80	18

Reuse of AIP Publishing content is subject to the terms at: https://publishing.aip.org/authors/rights-and-permissions. Download to IP: 143.54.44.137 On: Thu, 05 May 2016 19:14:47

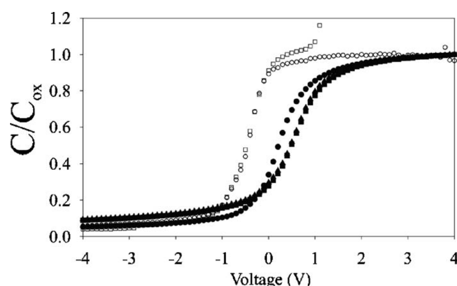

FIG. 3. HFCV measurements of all capacitors. Symbols are the same as in Fig. 1. The ideal flatband voltage (V_{fb}) is −0.16 V.

titative way, one notices the occurrence of both higher O isotopic exchange and N removal. These effects can be attributed to the harsher conditions of SiC anneals, namely, higher temperatures and longer annealing times. Besides, physicochemical differences between thermal oxides grown on Si and on SiC, like the presence of C,[2,6] could mediate different isotopic exchange mechanisms that are not present in the Si case.

Figure 3 shows the HFCV curves for all sets of MOS capacitors. The HFCV curve of NO samples (the same symbols as in Fig. 1) exhibits smaller negative flatband-voltage shift when compared to the gate oxides grown only in $^{18}O_2$ and in NO/$^{18}O_2$. The flatband-voltage shift from the ideal value (V_{fb}=−0.16 V) is caused by the charge on the interface traps and fixed oxide charge. $^{18}O_2$ samples also exhibit increased accumulation capacitance due to increased oxide leakage at the testing temperature. These results indicate that the gate dielectric/SiC interface is degraded whenever the $^{18}O_2$ annealing is performed last. The electrical degradation of the interface is attributed to the removal of Si–N bonds and/or formation of C clusters and silicon oxycarbides. Samples that underwent NO annealing last ($^{18}O_2$/NO and NO/$^{18}O_2$/NO), presented a moderate positive flatband-voltage shift. This can be explained by considering that the last NO annealing is leading to two competitive processes: passivation of the SiO_2/SiC interface by nitridation, improving the quality of the interface, and further oxidation of the SiC substrate. The positive flatband-voltage shift is originated[5] by the remaining active defects at the film/semiconductor interface, such as C clusters and silicon oxycarbides. No discernible differences between *C-V* curves of the $^{18}O_2$/NO and NO/$^{18}O_2$/NO samples were observed in this work, but lower slow-trap density and lower SiC surface microroughness due to the NO/$^{18}O_2$/NO route were reported.[8] Although NO samples present the best electrical characteristics, NO/$^{18}O_2$/NO samples are an interesting alternative for fabrication technology as they reduce significantly the long time consumed in gate dielectric growth in NO only.

In summary, we have investigated physicochemical and electrical properties of dielectric films thermally grown on SiC by different sequential thermal processing routes in NO and in O_2. Direct oxynitride growth in NO presented the best *C-V* characteristics. Oxidation in O_2 of NO annealed samples breaks Si–N bonds, releasing N that desorbs, while further film growth is induced, together with O isotopic exchange. *C-V* characteristics of these samples evidenced a degraded interface region probably due to removal of N and formation of C compounds during further substrate oxidation. A subsequent NO annealing step led to moderate positive flatband-voltage shift in *C-V* curves. This shift is related to the competitive process between electrical passivation and formation of electrically active C compounds. On the other hand, NO annealing performed after the SiO_2 film thermal growth in O_2 led to N incorporation, forming Si–N bonds near the dielectric/semiconductor interface. O incorporation was also observed, resulting in film growth and isotopic exchange between O atoms from the gas phase and those already existent in the dielectric film. *C-V* characteristics obtained are very similar to those obtained in the NO/O_2/NO route. Therefore, the initial nitridation step in NO in the NO/O_2/NO route yielded no significant improvements on the *C-V* characteristics as compared to the O_2/NO route, although improvements on other electrical characteristics are expected based on previously published results. Thus, in the search for dielectric films with improved electrical characteristics on SiC, the O_2/NO or NO/O_2/NO processing routes investigated here constitute alternatives for the lengthy gate dielectric growth in NO only.

The authors would like to thank CAPES, CNPq, FAPERGS, and ARC (Australian Research Council) for financial support.

[1] R. Singh, Microelectron. Reliab. **46**, 713 (2006).
[2] V. V. Afanas'ev, M. Bassler, G. Pensl, and M. Schulz, Phys. Status Solidi A **162**, 321 (1997).
[3] A. Ekoué, O. Renault, T. Billon, L. Di Cioccio, and G. Guillot, Mater. Sci. Forum **433**, 555 (2002).
[4] K. Fukuda, S. Suzuki, T. Tanaka, and K. Arai, Appl. Phys. Lett. **76**, 1585 (2000).
[5] S. Dahr, L. C. Feldman, S. Wang, T. Isaacs-Smith, and J. R. Williams, J. Appl. Phys. **98**, 014902 (2005).
[6] S. Wang, S. Dahr, S.-R. Wang, A. C. Ahyi, A. Franceschetti, J. R. Williams, L. C. Feldman, and S. T. Pantelides, Phys. Rev. Lett. **98**, 026101 (2007).
[7] P. Jamet, S. Dimitrijev, and P. Tanner, J. Appl. Phys. **90**, 5058 (2001).
[8] K.-Y. Cheong, S. Dimitrijev, and J. Han, Mater. Sci. Forum **433**, 583 (2002).
[9] K. McDonald, M. B. Huang, R. A. Weller, L. C. Feldman, J. R. Willians, F. C. Stedile, I. J. R. Baumvol, and C. Radtke, Appl. Phys. Lett. **76**, 568 (2000).
[10] I. J. R. Baumvol, Surf. Sci. Rep. **36**, 1 (1999).
[11] Z.-Q. Yao, J. Appl. Phys. **78**, 2906 (1995).
[12] H. Li, S. Dimitrijev, D. Sweatman, H. B. Harrison, P. Tanner, and B. Feil, J. Appl. Phys. **86**, 4316 (1999).
[13] I. J. R. Baumvol, J.-J. Ganem, L. G. Gosset, I. Trimaille, and S. Rigo, Appl. Phys. Lett. **72**, 2999 (1998).
[14] I. J. R. Baumvol, T. D. M. Salgado, C. Radtke, C. Krug, and J. de Andrade, Appl. Phys. Lett. **73**, 1970 (1998).

Reuse of AIP Publishing content is subject to the terms at: https://publishing.aip.org/authors/rights-and-permissions. Download to IP: 143.54.44.137 On: Thu, 05 May 2016 19:14:47